HHS Public Access

Author manuscript

Nat Neurosci. Author manuscript; available in PMC 2016 July 25.

Published in final edited form as:

Nat Neurosci. 2016 March ; 19(3): 465–470. doi:10.1038/nn.4224.

Separate Circuitries Encode the Hedonic and Nutritional Values of Sugar

Luis A. Tellez[1,2], **Wenfei Han**[1,2], **Xiaobing Zhang**[3], **Tatiana L. Ferreira**[1,2,4], **Isaac O. Perez**[1], **Sara J. Shammah-Lagnado**[5], **Anthony N. van den Pol**[3], and **Ivan E. de Araujo**[1,2,6,*]

[1]The John B Pierce Laboratory, New Haven CT, USA

[2]Department of Psychiatry, Yale University School of Medicine, New Haven CT, USA

[3]Department of Neurosurgery, Yale University School of Medicine, New Haven CT, USA

[4]Mathematics, Computing and Cognition Center, Federal University of ABC, Santo André SP, 09210, Brazil

[5]Department of Physiology and Biophysics, Biomedical Sciences Institute, University of São Paulo, São Paulo SP, Brazil

[6]Department of Physiology, Yale University School of Arts and Sciences, New Haven CT, USA

Abstract

Sugar exerts its potent reinforcing effects via both gustatory and post-ingestive pathways. It is however unknown if sweetness and nutritional signals engage segregated brain networks to motivate ingestion. We show in mice that separate basal ganglia circuitries mediate the hedonic and nutritional actions of sugar. We found that, during sugar intake, suppressing hedonic value inhibited dopamine release in ventral but not dorsal striatum, whereas suppressing nutritional value inhibited dopamine release in dorsal but not ventral striatum. Consistently, cell-specific ablation of dopamine-excitable cells in dorsal, but not ventral, striatum inhibited sugar's ability to drive the ingestion of unpalatable solutions. Conversely, optogenetic stimulation of dopamine-excitable cells in dorsal, but not ventral, striatum substituted for sugar in its ability to drive the ingestion of unpalatable solutions. Our data demonstrate that sugar recruits a distributed dopamine-excitable striatal circuitry that acts to prioritize energy seeking over taste quality.

*Corresponding Author: Ivan E de Araujo, The John B. Pierce Laboratory & Yale University School of Medicine, 290 Congress Avenue, New Haven CT 06519, USA, Phone: +1 (203) 5629901 x204, Fax: +1 (203) 6244950, ; Email: IAraujo@jbpierce.org, ; Email: ivan.araujo@yale.edu

Author Contributions IEA conceived the study. IEA and LAT designed experiments. LAT, WH, and TLF performed gastrointestinal and stereotaxic surgeries, performed behavioural/optogenetic experiments, performed microdialysis studies, and analysed data. WH, SJL and TLF performed histological analysis and imaging. XG and AvdP performed whole-cell patch clamp experiments, performed high-res imaging of brain slices, and analysed data. IOP and LAT performed *in vivo* electrophysiological experiments and analysed data. IEA wrote manuscript. All authors actively participated in interpreting all data and in manuscript editing.

Introduction

Unlike artificial sweeteners, sugar promotes ingestive behaviour via both gustatory and post-ingestive pathways[1–4]. However, the neural mechanisms mediating sugar's dual control over behaviour remain elusive. Specifically, it remains unknown if gustatory and post-ingestive signals recruit shared or segregated neural circuitries to promote intake. Overcoming our incomplete understanding of how calories modify the reward value of sweet substances should provide novel strategies for curbing excess sugar intake[4].

In the vertebrate brain, the striatal areas of the basal ganglia are crucial for selecting reward-based actions and evaluating their outcome[5–8]. Within the striatum, the anatomical segregation between dorsal and ventral regions is an evolutionarily conserved trait[9] previously linked to dissociable behavioural functions[6,10]. The execution of these anatomically specific behavioural functions critically depends, in turn, on striatal dopamine signalling[7,11,12]. We therefore investigated whether the distinction between gustatory *vs.* post-ingestive reward reflects the anatomical specialization between ventral *vs.* dorsal dopamine-controlled striatal sectors.

Results

Taste and nutrition separately control dopamine levels

We started by monitoring dopamine release in both ventral ("VS") and dorsal ("DS") striatal sectors during the active intake of nutritive and non-nutritive sweeteners. Briefly, mice licked a spout containing a non-caloric sweetener (*i.e.* sucralose), such that lick detection by the contact lickometer triggered intra-gastric infusions of solutions containing either sucralose or sugar (*i.e.* D-glucose). This procedure, performed concomitantly to brain microdialysis (Supplementary Fig. 1A–B), eliminates potential confounds associated with differences in taste quality/intensity between sugars and artificial sweeteners. We chose D-glucose to model sugar ingestion due to its unvarying presence in sugared products.

We observed increased dopamine release above baseline levels in VS during sweetener intake, irrespective of which solution was administered intra-gastrically (Figure 1A). However, dopamine release in DS increased above baseline levels only when sweetener intake was accompanied by intra-gastric infusions of glucose (Figure 1B), suggesting selective sensitivity of DS-projecting dopamine cells to sugar. We thus assessed the impact on dopamine release produced by lessening the hedonic value of the solutions. We achieved this by adulterating the sucralose solution with the bitter compound denatonium benzoate. In these experiments, licking the sweet/bitter stimulus was always accompanied by intra-gastric infusions of glucose. Intriguingly, while sweetener adulteration suppressed sugar-induced dopamine release in VS (which did not surpass baseline levels), evoked dopamine release remained similarly robust, rising above baseline levels in DS (Figures 1C and Supplementary Fig. 1C–D). Note that sugar-induced changes in dopamine levels failed to rise above baseline levels in VS despite the energy content of the solutions. Thus, while energy per se is capable of driving dopamine release in VS[3,13], taste quality gates this sugar-induced ventral dopamine efflux[14,15].

We then performed the reciprocal experiment by replacing (D-)glucose with its non-metabolizable enantiomer L-glucose: In these experiments, licking the sweet stimulus was accompanied by intra-gastric infusions of the non-metabolizable sugar. In striking symmetry with the previous experiment, whereas replacing D-glucose with L-glucose suppressed sugar-induced dopamine release in DS (which did not surpass baseline levels), sweetness-induced dopamine release remained similarly robust, rising above baseline levels in VS (Figures 1D and Supplementary Fig. 1E–F). Importantly, the observed sugar-induced changes in dopamine levels were not associated with licking rates *per se* (Supplementary Fig. 1G–H). In fact, intra-gastric infusions performed outside any behavioural context (*i.e.* in the absence of licking activity) produced sugar-induced increases in dopamine levels that were statistically indistinguishable from those observed during the behavioural sessions (Supplementary Fig. 1I–J). Furthermore, sugar-induced dopamine release did not require intra-gastric glucose to be a novel stimulus, nor did it evoke unspecific motoric activities (Supplementary Fig. 2). In sum, whereas taste quality regulates dopamine release in ventral striatum, increases in dopamine release in dorsal striatum are under strict metabolic control.

Increasing dopamine levels mimics taste and nutrition

We next analysed the functional implications of metabolism-driven dopamine release in DS. We found that hungry mice consume significantly more of the unpalatable solution when associated with intra-gastric sugar compared to intra-gastric artificial sweetener (Supplementary Fig. 3A–B). Consistent with a role for DS dopamine signalling in this phenomenon[6,10,11], perfusion of either VS or DS with dopamine via reverse microdialysis induced robust licking of the unpalatable solution (Supplementary Fig. 3C–D). In sum, hungry mice endure unpalatable solutions when those are associated with gut energy sensing, an effect mirrored by artificially increasing extracellular dopamine levels in DS and VS (thereby mimicking the effects of nutrition and sweetness on dopamine release).

D1r neurones in dorsal striatum drive nutrient seeking

We next tested whether striatal dopamine signalling mediates the functional organization of basal ganglia pathways in terms of hedonics *versus* nutrition. Since dopamine increases the excitability of D1r-expressing neurones[16,17], we specifically focused on their role in sugar reward. We first performed loss-of-function cell ablation studies. We achieved cell-specific ablation of D1r-neurones in DS or VS by virally introducing a *Cre*-dependent caspase into D1r-*Cre* mice. Specifically, the *Cre*-dependent viral construct AAV-flex-taCasp3-TEVp[18] was stereotaxically injected bilaterally into DS or VS of D1r-*Cre* mice. Non-*Cre* mice transfected with AAV-flex-taCasp3-TEVp were used as controls.

We first assessed the impact of cell-specific ablations on taste responses by employing brief-access licking tests[19]. Test stimuli consisted of a sucralose solution mixed to increasing levels of the bittering agent denatonium. We found that ventrally-ablated (“VS-casp”) mice were significantly more impacted by the lowest concentrations of denatonium, whereas dorsally-ablated (“DS-casp”) mice were similar to controls (“WT-casp”, Figure 2A). Similar results are obtained when increasing concentrations of sweetener are used to mask bitterness (Supplementary Fig. 3E). We then performed the converse experiment by presenting mice with a fixed bitter solution, and pairing licks to increasing concentrations of intra-gastric

glucose. When the concentration of the glucose infusate was low, VS-casp mice were again significantly more impacted by bitterness than DS-casp and WT-casp mice (Figure 2B). Now, upon increasing the concentration of the glucose infusate, both VS-casp and WT-casp control mice markedly increased responding only to reach similarly high levels; however, DS-casp mice failed to do so, remaining at their baseline levels (Figures 2B and Supplementary Fig. 3F). The lesion-specific differences then diminish upon infusions of more satiating intra-gastric loads (Supplementary Fig. 3F).

We inquired if the above phenomena generalizes to learned chemosensory cues by employing a taste-nutrient learning paradigm[1,2]. Naïve DS-casp, VS-casp, and WT-casp mice were initially tested on brief-access two-bottle preferences involving a sucralose solution and an unpalatable bitter/sweet mixture. Not surprisingly, all mice preferred to lick the sweet-only solution (Figure 2C). Next, mice were exposed to one-bottle learning sessions where licks for the sweet solution were paired to intra-gastric infusions of the non-nutritive sweetener. Then, on a different day, licks for the bitter/sweet solution were paired to intra-gastric infusions of the nutritive glucose. Two-bottle preference tests were performed again on a fourth testing day. All mice markedly shifted preferences towards the unpalatable nutritive stimulus, except DS-casp mice, which continued to prefer the non-nutritive but palatable solution (Figure 2D). In sum, VS and DS D1r-neurone populations separately mediate the gustatory and nutritional actions of sugar. Importantly, the lesions affected neither licking rates nor the amounts of intra-gastric sugar infused during conditioning (Supplementary Fig. 3G). Neuroanatomical criteria were employed to verify the specificity of the lesions (Figure 2E–H; Supplementary Fig. 3H–K shows the analyses of sham lesions).

Activating D1r neurones in dorsal striatum mimics sugar

We further explored the circuit basis of the above phenomena by performing optogenetic gain-of-function studies. Using slice electrophysiological recordings, we confirmed increased excitability of mouse D1r-expressing neurones in the presence of dopamine (Figure 3A–B). We thus tested the hypothesis that artificial activation of D1r-neurones in DS would substitute for sugar during ingestion of unpalatable adulterated sweeteners. Specific expression of the light-sensitive *Channelrhodopsin* (ChR2) in D1r-neurones was achieved by stereotaxically injecting the Cre-dependent viral construct AAV-EF1a-DIO-hChR2(H134R)-EYFP into the VS and DS of D1r-Cre mice[20,21]. Slice electrophysiological recordings confirmed robust excitation of D1r-neurones by 473nm laser pulses (Figures 3C and Supplementary Fig. 4). *Cre*-dependent expression of ChR2 was confirmed by neuroanatomical criteria (Figures 3D and Supplementary Fig. 5A–B).

During optogenetic experiments mice licked a spout containing sucralose such that detected licks triggered, instead of intra-gastric infusions, light pulses to VS or DS. While optogenetic stimulation of D1r-neurones in VS significantly enhanced sucralose licking, it failed to attenuate the suppressive effects produced by adulterating sucralose with denatonium (Figure 3E). The ability of VS stimulation to drive intake thus depends on the hedonic properties of the stimulus, and suggests the involvement of alternative circuits in intake suppression. However, stimulation of D1r-neurones in DS not only increased intake of sucralose, but also completely annulled the suppressive effects produced by the bitter toxin

(Figure 3F and Supplementary Movie 1). Importantly, this was not due to altered taste perception upon light activation (Supplementary Fig. 6A), or to ceiling effects (Supplementary Fig. 6B–E). Optical activation induced self-stimulation (Supplementary Fig. 6F–H) but not increased locomotor activity (Supplementary Fig. 6I). Moreover, optical activation did not alter the animals' sensitivity to either satiety or aversive sensory stimuli (Supplementary Fig. 6J–K). These data suggest that optical stimulation did not disrupt goal-direct action by inducing unspecific insensitivity to devaluation. In sum, D1r-neurone stimulation in DS, but not VS, substituted for sugar in its ability to drive ingestion of unpalatable stimuli.

Additionally, using a conditioned taste aversion paradigm, we found that DS, but not VS, D1r-neurone stimulation overrode unpalatability produced by associating a novel sweetener (Rebaudioside A) to visceral malaise (Figure 3G). Thus, unpalatability resulting from either innate bitterness or learned sickness is consistently overridden by DS stimulation. Remarkably, such disparities in VS and DS response patterns appear to be limited to contexts associated with food intake: using a nose-poke-based protocol[20], we found equally potent D1r-neurone self-stimulation in both regions (Figure 3H).

In addition to increasing excitability of striatal D1r-neurones, dopamine concomitantly diminishes excitability of D2r-neurones[16,17]. In fact, D2r-neurones cooperate with D1r-neurones to control goal-directed actions[22] and play a critical role in compulsive eating[23]. We therefore investigated the effects of optogenetically inhibiting D2r-neurones on the intake of both the sweet and adulterated solutions. Interestingly, inhibition of D2-neurones in VS slightly enhanced licking of the sweet solution without attenuating the aversive effects of adulteration by bitterness (Supplementary Fig. 5C). Inhibition of D2-neurones in DS, in contrast, did not affect licking of sweet solutions and only slightly attenuated adulteration effects (Supplementary Fig. 5D). Thus, unlike the case of D1r-neurone stimulation, unpalatability was not fully overridden by D2r-neurone inhibition. We note however that the above does not rule out an important role for D2r-neurones in controlling sugar ingestion. Future experiments must determine the effects on intake of ablating D2r-neurones in striatum.

D1r neurones in dorsal striatum override taste aversion

The major projections of DS D1r-neurones are to the entopeduncular nucleus and the *pars reticulata* of *Substantia nigra* (SNr). Because SNr is preferentially responsive to oral-facial movements[24], this target was chosen for optic and chemogenetic manipulations. In contrast, a major outflow of VS D1r-neurones is directed to the ventral pallidum (VP). These DS and VS D1r-targets are consistent with *ChR2* terminal labelling (Figure 3D). Now, because DS and VS D1r-neurones are GABAergic[7,9], the net outcome of stimulating D1r-striatal neurones is the inhibition of their downstream targets[25]. We therefore reasoned that optogenetic activation of SNr and VP would counteract the effects of stimulating DS and VS, respectively.

Consistent with an inhibitory tone exerted by VS and DS on VP and SNr, respectively, optogenetic activation of VP indiscriminately suppressed sweet intake, whereas the inhibitory effects produced SNr activation were gated by the presence of sugar in gut

(Supplementary Fig. 7). These results provide initial support for the concept that sugar stimulation of dorsal pathways drives intake independently of the dopaminergic state of ventral pathways.

We thus explicitly tested the hypothesis that the dorsal DS=>SNr pathway controls sugar intake independently of the sweetness-sensitive VS=>VP ventral pathway. We employed a combination of optogenetics and chemogenetics[26]. One group of animals was ChR2-tranfected in VS, and optical fibres placed immediately above the D1r-neurone terminals in VP. A second group of animals was ChR2-tranfected in DS, and optical fibres placed immediately above the D1r-neurone terminals in SNr. To reversibly increase activity levels in the ventral output station, animals in both groups were stereotaxically injected with the construct AAV-hSyn-HA-hM3D(Gq)-IRES-mCitrine in VP (preparation illustrated in Supplementary Fig. 8).

In vivo neuronal activation and slice electrophysiology measures confirmed that D1r-positive VS terminals inhibit their VP targets via GABAergic mechanisms (Supplementary Fig. 9). We found that, in the absence of light pulses, administering the designer drug clozapine-N-oxide (CNO) robustly suppressed sweetener intake in both DS and VS-implanted animals (Figure 4A). Consistently, optogenetic activation of VS=>VP terminals produced an increase in sweetener intake that was blocked by activating VP with CNO (Figure 4B, red). However, activating VP with CNO produced no inhibitory effects on the robust increases in sweetener intake associated with optogenetically activating DS=>SNr terminals (Figure 4B, blue). Stimulation of dorsal pathways is therefore sufficient to override suppressive commands associated with VP activation. These effects are pathway-specific: when animals expressed hM3D(Gq) in SNr, CNO administration effectively inhibited increases in intake associated with optogenetic activation of DS=>SNr terminals (Figures 4C). Consistent with our overall model, optogenetic activation of DS=>SNr terminals strongly stimulated the intake of the unpalatable bitter sugar solution, an effect partially blocked by CNO administration (Figure 4D). Reliable activation of hM3D(Gq)-transfected neurones in VP and SNr was confirmed *in vivo* using early gene and multi-channel electrophysiological measurememts (Figures 4E–F and Supplementary Figs. 10–11). Overall, these results reveal that the dorsal DS=>SNr pathway operates, to a large extent, independently of the (ventral) VS=>VP pathway.

Discussion

Our data imply a model for sugar reward where hedonic and metabolic positive controls on intake are encoded and mediated by separate sensorimotor circuits. We found in vertebrates that the dorsal, but not ventral, basal ganglia descending pathway is recruited only when energy is present in a sweet solution. Importantly, the activation of dorsal pathways is sufficient to override inhibitory signals generated by ventral pathways during the ingestion of aversive substances. Such circuit logic implemented in the striatum allows the organism to prioritize energy seeking over sensory quality.

This general trait appears to be conserved in invertebrates: *Drosophila* flies favour metabolizable over non-metabolizable sugars independently of sweet receptor activity[27].

Consistently, dopaminergic signalling mediates the ability of *Drosophila* to determine the nutritional value of sweet tastes[28], to the extent that separate dopamine neurones mediate the mnemonic encoding of gustatory and nutritional cues[29]. The separation of gustatory and post-ingestive reinforcement at the dopaminergic circuitry level thus emerges as an evolutionary conserved trait affecting both vertebrate and invertebrates.

We found that this dopaminergic circuitry responds to intra-gastric infusions of sugar independently of any behavioural requirements (Supplementary Figure 1I–J). The question thus arises of how dopamine receptor signalling may assign "value" to the sugar stimulus. To resolve this apparent inconsistency, we first define the equivocal term "value"[30]. We interpret "value" as a stimulus property whose detection by the nervous system is sufficient to alter the probability of subsequent responding to this stimulus. The assignment of hedonic/nutritional "value" to the sugar stimulus is thus operationally defined by the augmenting effect of gustatory/post-ingestive signals on the probability of responding. This is functionally equivalent to the standard interpretation of "value" in behavioral neuroscience, where the term refers to the motivating properties of a stimulus for instrumental action[30]. Consistently, we found that while gut-induced dopamine release constitutes a physiological reflex, such reflex alters the probability of responding by recruiting downstream dopamine-excitable cells in striatum (Figures 2,3). This gut-triggered mechanism thereby supports the assignment of "value" to sweet solutions. The same effect promptly extends to Pavlovian values[30], as demonstrated by taste-nutrient conditioning studies (Figure 2C–D). Overall, nigrostriatal dopamine cells may be conceptualized as sensorimotor interneurons linking physiological nutrient sensing to the assignment of "value" to goal-directed actions and sensory stimuli.

At least one fundamental issue remains nonetheless unaddressed. According to the model delineated above, nutritional control over intake must ultimately translate into oral-motor consummatory patterns. Our studies support a mechanism via which, upon sugar intake, metabolic cues act on D1r-expressing neurones in dorsal striatum to selectively bias goal-directed action. We postulate that this is achieved via the release of brainstem oral-motor centres from tonic inhibition by SNr[25]. Our model specifically predicts that the descending pathway from SNr to the premotor reticular formation[31] links nutrient sensing in basal ganglia to the execution of feeding motor programs (Supplementary Fig. 12). Future research must determine the molecular identity of the circuitry that links energy sensing in forebrain to the motor central pattern generators implemented in brainstem.

METHODS

Subjects

A total of 170 adult male mice were used, including 74 C57BL6/J wild-type mice, 68 D1-dopamine receptor Cre-recombinase male mice (*Drd1a-cre*$^{+}$, strain EY262, Gensat), 12 D2-dopamine receptor Cre-recombinase mice (B6.FVB(Cg)-Tg(Drd2-cre)ER44Gsat/Mmcd, Gensat) and 16 Ai32 mice (B6.Cg-*Gt(ROSA)26Sor*$^{tm32(CAG-COP4*H134R/EYFP)Hze}$/J, Jackson Laboratory). At the time of experiments animals were 8–20 weeks old, and had no previous experiences with any of the experimental conditions. All animals were group housed (<4 cage) previous to the beginning of experimental sessions. After randomized

assignment to an experimental group, all animals were housed individually. Animals were housed under a 6AM/6PM light/dark cycle. Experiments were performed consistently between 4PM-12AM to maximize motivation for feeding behaviour. Each individual animal was exposed to one single experimental group. All experiments were conducted in accordance with the J.B. Pierce Laboratory and Yale University regulations on usage of animals in research.

Surgical procedures

Gastric catheter implantation—Once animals had been anaesthetized with an I.P. injection of a ketamine/xylazine (100/15 mg kg^{-1}), a midline incision was made into the abdomen. The stomach was exteriorized through the midline incision and a purse string suture was placed in its non-glandular region, into which the tip of MicroRenathane tubing (Braintree Scientific Inc., Braintree, MA, USA) was inserted. The purse string was tightened around the tubing, which was then tunnelled subcutaneously to the dorsum via a small hole made into the abdominal muscle; a small incision to the dorsum between the shoulder plates was then made to allow for catheter exteriorization. Incisions were sutured and thoroughly disinfected and the exterior end of the catheter was plugged.

Microdialysis guiding cannulae implantation—For animals used in the microdialysis experiments, anesthesia was induced with I.P. injection of a ketamine/xylazine (100/15 mg kg^{-1}) and the mouse was placed on a stereotaxic apparatus (David Kopf, Tujunga, CA, USA) under constant flow of 1% isoflurane anaesthesia (1.5 l min^{-1}). For the dorsal striatal region a circular craniotomy was drilled at AP = 1.0 mm and ML =±1.7 mm implantation of a guide cannulae (DV = −2.0 mm from skull surface) for posterior insertion of a microdialysis probe whose exposed dialysis membrane was 2mm high; for the ventral striatal region a circular craniotomy was drilled at AP = 1.5 mm and ML =±0.6 mm implantation of a guide cannulae (DV = −4.0 mm from skull surface) for posterior insertion of a microdialysis probe whose exposed dialysis membrane was 1mm high.

Viral delivery of transgenes—Adeno-associated viruses (AAVs, serotype 5, University of North Carolina Vector Core) carrying genes of interest were obtained from the University of North Carolina Vector Core Services. All injections were bilateral into the structure of interest. For Cre-dependent transfection with the blue light-sensitive ion channel channelrhodopsin (ChR2), the construct AAV-EF1a-DIO-hChR2(H134R)-EYFP was used. For Cre-dependent transfection with a green light-sensitive archeorhodopsin (eArch3.0), the construct AAV-EF1a-DIO-eArch3.0-EYFP was used. For combination with chemogenetic stimulation (DREADDs), AAV-hSyn-HA-hM3D(Gq)-IRES-mCitrine was also injected in the relevant site and receptors activated by clozapine-N-oxide at 1mg/kg ip. Control animals were of the corresponding strain, transfected with a light-insensitive Cre-dependent ion channel (AAV-hSyn-DIO-HA-hM3D(Gq)-IRES-mCitrine). For *Cre*-dependent caspase-mediated ablation of dopamine-excitable neurons in striatum, the *Cre*-dependent viral construct AAV-flex-taCasp3-TEVp was used. All procedures, including fiber placement and laser activation, were identical for ChR2+ and ChR2- mice.

Caspase-mediated ablation of dopamine-excitable cells: To achieve *Cre*-dependent caspase-mediated ablation of dopamine-excitable neurons in striatum, the *Cre*-dependent viral construct AAV-flex-taCasp3-TEVp (serotype 5, University of North Carolina Vector Core) was stereotaxically injected (0.5 μL per hemisphere) into the dorsal or ventral striatum of D1r-*Cre* mice at same coordinates used for optogenetic experiments. The two control groups included D1r-*Cre* mice transfected with AAV5-GFP constructs, and non-*Cre* mice transfected with AAV-flex-taCasp3-TEVp. Cell-specificity of the ablations was confirmed via neuroanatomical retrograde tracing methods. The fluorescent retrograde tracer Red Retrobeads (LumaFluor) was injected into the *Substantia Nigra, pars reticulata* (0.1μl), the exclusive ipsilateral target of D1r-expressing neurons of dorsal striatum on one hemisphere, and into the *Globus Pallidus* (0.1μl), the exclusive ipsilateral target of D2r-expressing neurons of dorsal striatum, on the other hemisphere. It was then confirmed, using fluorescent microscopy, the strong labeling throughout dorsal striatum on the same hemisphere in which the retrograde fluorescent beads were injected into *globus pallidus*, and weaker labeling throughout dorsal striatum on the same hemisphere in which the retrograde fluorescent beads were injected into *Substantia Nigra pars reticulata.* Equivalent Retrobead injections were made into the ventral pallidum, the preferential target of ventral striatal D1r-expressing neurons. To allow visualization of the relevant anatomical landmarks, images show the Retrobead fluorescence signal overlaid on a bright field image of the same section.

Stereotaxic viral injections and optic fibres implantation—For animals used in the optogenetics experiments, anaesthesia was induced with an I.P. injection of a ketamine/xylazine (100/15 mg kg^{-1}) and the mouse was placed on a stereotaxic apparatus (David Kopf, Tujunga, CA, USA) under constant flow of 1% isoflurane anaesthesia (1.5 l min^{-1}). All viral injections were done bilateral, using modified microliter syringes (Hamilton) with a 22 needle gauge. The tip of the needle was placed at the target regions and the injections were performed at a rate of 0.1μL min^{-1} (for coordinates and volumes see below). Once the injection was finished the needle was left in place for 10 min and then slowly removed. Immediately after the viral injection the optic fibres were implanted (200 μm core, 0.22NA, Doric Lenses). To allow time for viral expression, animals were housed for at least 2 weeks following injection before any experiments were initiated.

Drd1a- and *Drd2-cre* mice were used for injections at the dorsal and ventral striatal regions. The coordinates used for dorsal striatum were AP = 1.0 mm, ML =±1.7 and DV = −3.0 mm (from skull surface) and 1 μL of AAV-EF1a-DIO-hChR2(H134R)-EYFP virus was injected per hemisphere. The coordinates used for ventral striatum were AP = 1.5 mm, ML =±0.6 and DV = −4.5 mm (from skull surface) and 0.5 μL of either the AAV-EF1a-DIO-hChR2(H134R)-EYFP or AAV-EF1a-DIO-eArch3.0-EYFP viruses was injected per hemisphere.

Ai32 mice, which express a channelrhodopsin-2/EYFP fusion protein upon exposure to Cre recombinase, were used for ChR2 expression in ventral pallidum and *Substantia Nigra pars reticulata* regions. The coordinates used for ventral pallidum were AP = 0.7 mm, ML =±1.0 and DV = −4.9 mm (from skull surface). The coordinates used for *Substantia Nigra reticulata* were AP = −3.2 mm, ML =±1.6 and DV = 4.4 mm (from skull surface). In both cases 0.5 μL of AAV-CMV-Cre virus was injected per hemisphere.

Drd1a-cre mice were used for the experiments involving the simultaneous activation of striatal regions (dorsal and ventral) and their downstream targets (*Substantia Nigra pars reticulata* and ventral pallidum, respectively). AAV-EF1a-DIO-hChR2(H134R)-EYFP virus was injected in the striatal regions and AAV-hSyn-HA-hM3D(Gq)-IRES-mCitrine virus was injected in the downstream targets. The coordinates and volumes employed were the same as described before for the corresponding areas.

Stereotaxic viral injections and electrode array implantation—*Drd1a-cre* mice were used for the extracellular recording experiments, anaesthesia was induced with I.P. injection of a ketamine/xylazine (100/15 mg kg^{-1}), a small incision was made into the abdominal muscle and 3 cm MicroRenathane tubing was inserted in to the intraperitoneal cavity. The purse string was tightened around the tubing, which was then tunnelled subcutaneously to the dorsum via a small hole made between the shoulder plates to allow for catheter exteriorization. Immediately after, the mouse was placed on a stereotaxic apparatus (David Kopf, Tujunga, CA, USA) under constant flow of ~1% isoflurane anaesthesia (1.5 l min^{-1}) for viral injections and electrode implantation. AAV-hSyn-HA-hM3D(Gq)-IRES-mCitrine virus was then injected either in substantia nigra compacta or ventral pallidum. The procedure for the virus injection was the same as described before. Once the virus injection was completed, an electrode array consisting of 16 tungsten microwires (35-μm diameter) targeting substantia nigra compacta or ventral pallidum was implanted. Locations of electrodes were confirmed histologically.

Slice electrophysiology

On the day of the experiments, Drd1a-cre mice with selective ChR2 expression in striatal D1r neurons were anesthetized with isoflurane and decapitated for electrophysiological identification of striatal D1r-neurones and circuit mapping. Brains were quickly removed and immersed in an ice-cold high-sucrose solution containing (in mM): 220 sucrose, 2.5 KCl, 6 MgCl2, 1 CaCl2, 1.23 NaH2PO4, 26 NaHCO3, and 10 glucose (gassed with 95% O2 / 5% CO2; 300–305 mOsm). Coronal brain slices 300 μm thick were sectioned using a vibratome. Brain slices were then transferred to an incubation chamber filled with an artificial CSF (ACSF) solution containing (in mM) 124 NaCl, 2.5 KCl, 2 MgCl2, 2 CaCl2, 1.23 NaH2PO4, 26 NaHCO3, and 10 glucose (gassed with 95% O2 / 5% CO2; 300–305 mOsm) at room temperature (22 °C). After a 1–2 hrs recovery period, slices containing striatum, VP or SNr were selected and transferred to a recording chamber mounted on a BX51WI upright microscope (Olympus, Tokyo, Japan). The recording chamber was perfused with a continuous flow of gassed ACSF. A dual-channel heat controller (Warner Instruments, Hamden, CT) was used to control the temperature of recording solution at 33 ± 1 °C. Whole-cell patch-clamp recordings were performed on striatum D1r neurons and neurons in VP and SNr that were visualized using an infrared-differential interference contrast (DIC) optical system combined with a monochrome CCD camera and a monitor. Pipettes were pulled from thin-walled borosilicate glass capillary tubes (length 75 mm, outer diameter 1.5 mm, inner diameter 1.1mm, World Precision Instruments, Sarasota, Fl) using a P-97 micropipette puller (Sutter Instruments, Novato, CA). Pipette solution containing (in mM) 145 K-gluconate, 1 MgCl2, 10 HEPES, 1.1 EGTA, 2 Mg-ATP, 0.5 Na2-GTP, and 5 Na2-phosphocreatine (pH 7.3 with KOH; 290–295 mOsm) were used for whole-cell

recording. The pipettes of resistances ranging from 3 to 6 MΩ were used for experiment. EPC-10 patch-clamp amplifier (HEKA Instruments, Bellmore, NY) and PatchMaster 2.20 software (HEKA Elektronik, Lambrecht/Pfalz, Germany) were used to acquire and analyze data. Pipette and cell capacitance were compensated during experiment and neurons which the series resistance was >20 MΩ and changed >15% were excluded from the statistics. Traces were processed using Igor Pro 6.36 (Wavemetrics, Lake Oswego, OR). Inhibitory postsynaptic currents were recorded at the holding potential of −40 mV. An LED array (BXRAC2002, Bridgelux, Livermore, CA) was used to evoke the stimulation for optogenetic activation of ChR2 channels in brain slices. Continuous stimulation and stimulation of 10 ms duration with different frequency (1, 5, 10 or 20 Hz) were used in the experiment to test photostimulation-evoked response.

Stimuli and behavioural apparatus

The following taste stimuli were used as stated in the corresponding experiments:

2mM sucralose, a mixture of 3mM denatonium benzoate and 2mM sucralose (sweet/bitter mixture) and 3mM Rebaudioside A. 2mM sucralose, and L and D-glucose solutions at a concentration of 50% (w/v) were used for the intra-gastric infusion coupled to oral intake experiments. All reagents were obtained from Sigma-Aldrich and prepared fresh in distilled water.

Feeding/Licking experiments were conducted in either one of three identical mouse behaviour chambers enclosed in a ventilated and sound-attenuating cubicle (Med Associates Inc., St. Albans, VT, USA). Each chamber was equipped with a slot for sipper tubing placement located in the centre of one of the walls and hidden by a software-controlled door, which was opened at the beginning of the sessions. From then on licking was voluntary and the animals were allowed to initiate or interrupt licking *ad libitum*. The sipper was connected to a contact-based lick detection device allowing for measurements of licking responses with 10 ms resolution. All lick timestamps were saved in a computer file for posterior analysis. Software controlled lasers and infusion pumps equipped with TTL input devices were connected to the behavioural chambers and programmed to automatically trigger laser and/or infusions in response to the detection of licks. MED-PC® IV (Med Associates Inc., St. Albans, VT, USA) was used as the platform for programming all experiments.

Behavioural sessions

Prior to obtaining the final behavioural test, animals were habituated to the behavioural boxes and the experimental conditions during five daily 1 h sessions.

i. Animals used for the extracellular dopamine measurements were trained to drink sucralose while receiving an intra-gastric infusion of sucralose. The exterior part of the gastric catheter was connected to a segment of MicroRenathane tubing secured to the tip of a 3mL standard syringe containing the solutions to be infused and mounted on the syringe pump. The syringe pump was placed near a small hole made on the superior part of the sound attenuating box in such a way that mice were able to move freely inside the behavioural chambers. During the task, a

detected lick triggered an intra-gastric infusion that lasted 3 seconds (at a rate of 0.6mL min^{-1}; 30μL/infusion). Licks detected while an infusion was taking place had no programmed consequences. In order to get the animals used to the microdialysis settings, during these sessions the mice were also connected to dummy microdialysis probes. All sessions lasted for 1 hour. During the experimental session, the drinking solution and the syringe content were changed according to the different experimental conditions.

Mice exposed to the bitter-triggered intra-gastric infusions were exposed to these experimental conditions for three daily sessions before the dopamine measurements were performed (numbers of licks in each case: Habituation Day 1: 160±22, Habituation day 2: 162±13, VS or DS microdialysis day (*i.e.* day 3 or 4, counterbalanced): 118±14 or 131±23, repeated–measures one-way ANOVA across testing days $F[3,15]=0.92$, $p=0.45$. All paired t-tests involving the number of licks during microdialysis versus habituation $p>0.25$). The bitter solutions were never present in any of the intra-gastric infusates in any condition, only in solutions available for licking.

ii. Animals used for the optogenetic experiments were first trained to drink 2mM sucralose while plugged to the optic fibres but without receiving blue light pulses: and then later the drinking solutions and light stimulation were changed according to the different experimental conditions. To couple consumption to laser activation, detected licks triggered a 473nm blue laser source via TTL pulses as described in our previously for intra-gastric infusions. Intensity at tip of fibres was estimated at approximately 5mW. Constant pulses of light were used for D1 stimulation lasting 0.5 seconds, whereas 10Hz pulses lasting 1s were used for ventral pallidum and subtantia nigra reticulata stimulation. Licks detected while the laser was on had no programmed consequences. In the D1- stimulation experiments were licking was coupled to intra-gastric infusions, the duration of the light pulses was the same than the infusions (constant light pulses lasting 3s). All stimulations were performed bilaterally.

iii. Conditioned taste aversion. On the first session D1-Cre mice were exposed for 30 minutes to a new tastant (the artificial sweetener Rebaudioside A) and 15 min after the end of the session the animals received an I.P. injection of the malaise-inducing agent lithium chloride (0.35 M, 10 μl/g body weight). On the following day, conditioned aversion was tested. During this 30 minutes session, all groups received a 1s light pulse per every 20 licks produced. Licks detected while the laser was on had no programmed consequences. All stimulations were performed bilaterally.

iv. Nose poke task. Mice were placed in an operant box equipped with two slots for nose pokes at symmetrical locations on one of the cage walls. Nose pokes were connected to a photo-beam detection device allowing for measurements of responses with 10 ms resolution, and only one of them triggered the laser (1 second constant stimulation). The active side was counterbalance among animals and responses detected while the laser was on had no programmed consequences. Two

consecutive days of stimulation sessions were done and on the third day one extinction test was performed (meaning both nose pokes were inactive). All responses timestamps were saved in a computer file for posterior analysis. All experimental sessions were 30 min long. The preference ratio was calculated as follows:

$$Preference\ ratio\ for\ active\ side = n(active\ side)/[n(active\ side) + n(inactive\ side)]$$

where *n* denotes the detected number of responses for the corresponding side during a given session.

v. Opto and chemogenetic experiments. Clozapine N-oxide was dissolved in saline to a concentration of 0.1 mg ml^{-1} and injected I.P. 25 min before the beginning of the behavioural sessions. CNO was administered to each mouse (1mg kg^{-1} body weight). During the behavioural sessions licks triggered the laser as described before (1 second constant stimulation).

vi. To assess if D1-stimulation had an effect on the taste perception we performed short-term two-bottle preference tests. These experiments were carried out in a chamber equipped with two slots for sipper tubing placements, at symmetrical locations on one of the cage walls. Both sippers were connected to a contact-based lick detection device allowing for measurements of licking responses and responses produced in both sippers triggered the laser (0.5 seconds constant stimulation). One of the sippers contained sucralose and the other the bitter mixture. To eliminate the influence of side-biases, mice were tested for four consecutive sessions with the content of the sipper being switched across session. All sessions lasted for 10 min. Preference ratio for sucralose was calculated as described before for the nose pokes.

vii. For intra-gastric preloads, volume was determined from the averaged infused volume across animals during habituation (~0.75mL glucose; the same volume was used for sucralose preloads). Preload infusions were performed 10min previous to behavioural tests, at 0.1 mL min^{-1} infusion rate. During behavioural testing, the animals were allowed to drink and self-infuse as described above. Sessions lasted for 1 hour.

Nose-poking for obtaining food pellets—The same apparatus above was used in a goal-directed task in which mice were trained to poke on the active hole to obtain sugared food pellets (0.02g, BioServe). Four consecutive days of training sessions were performed, after which all mice showed high preferences for the active hole (see Extended Figure 2 for details). On the fifth and sixth days the tests were performed after an intra-gastric preload infusion of glucose or sucralose. Preload volume was determined from the averaged infused volume across animals during behavioural sessions (~0.75mL glucose; the same volume was used for sucralose preloads). Preload infusions were performed 10min previous to behavioural tests, at 0.1 mL min^{-1} infusion rate. Sessions lasted for 1 hour or 30 rewards earned, whatever the first occurrence.

The preference ratio for the active hole was calculated as above:

$$Preference\ ratio\ for\ active\ side = n(active\ side)/[n(active\ side) + n(inactive\ side)]$$

Outcomes were also quantified as rewards earned for further analyses.

Brief access tests—These tests were performed to assess if cell-specific ablation of D1r-neurones in DS or VS impact on hedonic responses as measured in classical brief-access tests. In these sessions, the licking spout was composed of four 20-gauge stainless-steel needles cemented together to prevent the mixing of the solutions; each needle was connected to a solenoid valve which in turn was connected to 50mL syringes containing the solutions employed in the corresponding session. Onset of the first trial is signaled by the vertical lifting of a sliding door within the behavioral apparatus described above. Only a single sipper, located behind the sliding door, was available in these sessions. The opening/closing of one of four solenoid valves was calibrated to deliver 5-μl drops of liquid, such that taste delivery was triggered by the detected licks. Each trial lasted for 5s from the time of the first detected lick, after which the sliding door is lowered. The taste stimuli were randomized across trials. Each session lasted for 20min. The following variations were performed:

Tolerance to bitter. Mixtures employed were: 1. 2mM Sucralose + 0.5mM Denatonium; 2. 2mM Sucralose + 1.5mM Denatonium; 3. 2mM Sucralose + 3.0mM Denatonium; and 4. 2mM Sucralose + 6mM Denatonium.

Masking bitterness. Mixture employed were: 1. 2mM Sucralose + 6mM Denatonium; 2. 4mM Sucralose + 6mM Denatonium; 3. 6mM Sucralose + 6mM Denatonium; and 4. 8mM Sucralose + 6mM Denatonium.

Sweetness. The taste stimuli employed were: 1. 0.5mM Sucralose; 2. 2mM Sucralose; 3. 4mM Sucralose; and 4. 6mM Sucralose.

Sugar-driven consumption of unpalatable solutions—To assess if cell-specific ablation of D1r-neurones in DS or VS impacts on the acceptance of unpalatable solutions instrumentally coupled to intra-gastric of D-glucose, the following experiment was performed. Mice were exposed to bitter-triggered intra-gastric infusions of four different D-glucose concentrations (0.5%, 10%, 25% and 50%), each one presented in independent sessions. Glucose concentration was randomized across mice and sessions. All sessions lasted 1h.

Taste-Nutrient Conditioning—First, short-term (5 min) two-bottle preference tests between sucralose and the bitter mixture were used to determine the short-term, oral relative preferences for each of these compounds before and after conditioning. To eliminate the influence of side-biases, mice were tested for two consecutive sessions with the content of the sipper being switched across sessions, and the outcome averaged. Conditioning sessions consisted of two separate 1 h one-bottle sessions. In one session, sucralose licks triggered intra-gastric infusions of sucralose. In a different session (on the next day), licks to the bitter mixture triggered intra-gastric infusions of D-glucose. The order of the conditioning sessions was counterbalanced across mice. On the following day after the second

conditioning, session, the two-bottle preference tests were repeated as above. Preference ratios for sucralose were calculated as described for the nose pokes.

Open field tests—To assess locomotor activity in response to our treatments, animals were placed on a novel Plexiglass arena (Med-Associates, 25cm×30cm). The total area was divided into 9 equal rectangular subareas (8.3×10cm), demarcated with yellow tape. Immediately above the central subarea a 150W lamp was activated to induce natural aversion to this particular location, as usually performed. Animals were tested once in this arena. The 10-min sessions were digitally recorded with a Sony HDR-CX440 camera. Data were analysed by replaying the sessions in slow-motion. Outcomes were the number of sequential crossings over *different* adjacent yellow lines (representing total locomotor activity), and relative time spent within the illuminated central part of the arena. In sessions involving intra-gastric preloads, preload volume was determined from the averaged infused volume across animals during previous behavioural sessions (~0.75mL glucose; the same volume was used for sucralose preloads). Preload infusions were performed 10min previous to behavioural tests, at 0.1 mL min^{-1} infusion rate. In sessions involving optical stimulation, laser source was continuously on throughout the session at intermittent ON/OFF intervals of 30sec, such that a randomization was performed to determine whether the laser source would be on during any particular 30 sec interval.

Control mice for optogenetics experiments—To control for genetic background, Chr2-independent light stimulation effects, and Cre-driven membrane receptor expression, D1-Cre mice were injected with the DREADD construct AAV-hSyn-HA-hM3D(Gq)-IRES-mCitrine and implanted with optical fibres exactly as ChR2-transfected mice. This thus produced *Cre*-dependent expression of a light-insensitive receptor in striatum. We observed that light pulses had no effects whatsoever on these animals and therefore omitted these data from main figures (where differential effects of VS *vs.* DS stimulation are shown, thereby evidencin light-independent effects) for simplicity. For completion however we show that light pulses produced no effects whatsoever on self-stimulatory rates in control mice, in stark contrast to VS and DS ChR2+ mice in which D1-neurone self-stimulation was highly rewarding (See Extended Data Figure 7).

Analyses of optically-triggered licking activity—Lifting vertically sliding door within the behavioral apparatus above signaled the beginning of a new trial. In each trial, the laser source was TTL-activated and left on during intervals of 1, 3, 5 or 7 seconds upon the detection of 13 consecutive licks to the sipper located behind the sliding door. A lick produced while laser source was on did not produce further stimulation. The length of stimulation was randomized across trials. Each trail lasted for 15s and the timer of the trial started to run after the laser was turned on. The sessions lasted for 1h.

Dopamine measurements during behaviour

During the experimental sessions, microdialysate samples from these freely moving mice were collected, separated and quantified by HPLC coupled to electro-chemical detection methods (‘HPLC-ECD’). Briefly, after recovery from surgery and habitation to the behavioural chambers, a microdialysis probe (CMA-7, cut off 6 kDa, CMA Microdialysis,

Stockholm, Sweden) was inserted into the striatum through the guide cannula (the corresponding CMA-7 model). After insertion, probes were connected to a syringe pump and perfused at 1.2 μl min^{-1} with artificial cerebrospinal fluid (aCSF; Harvard Apparatus, Holliston, MA, USA). After a 40 min washout period and a subsequent 30 min pre-intake baseline sampling, dialysate samples were collected every 10 min and immediately manually injected into a HTEC-500 HPLC unit (Eicom, Japan). Analytes were then separated via an affinity column (PP-ODS, Eicom), and compounds subjected to redox reactions within an electro-chemical detection unit (amperometric DC mode, applied potential range from 0 to 2000 mV, 1 mV steps). Resulting chromatograms were analysed using the software EPC-300 (Eicom), and actual sample concentrations were computed based on peak areas obtained from a 0.5 pg μl^{-1} dopamine standard solution (Sigma) and expressed as percentage changes with respect to the mean dopamine concentration associated with the baseline (i.e. pre-behavioural task) sampling period. Locations of microdialysis probes were confirmed histologically.

Reverse microdialysis—Reverse microdialysis was used to perfuse DS or VS with dopamine during ingestion of sucralose or sucralose+bitter. Licks were not followed by intra-gastric infusions in these experiments. Concentrations of the perfusates were chosen based on the average baseline dopamine levels previously observed with forward microdialysis, and increased 5 times to account for dilution (DS[DA]= 1.75 μg/mL = 9.22 μM; VS[DA]= 0.6 μg/mL =3.16 μM). Control sessions were identical except that only artificial cerebral spinal fluid (aCSF, Harvard Apparatus) was perfused. Perfusion rate was 1.5 μL/min. After a washout period of 40 minutes, mice were placed in the behavioral boxes while continuously perfused with aCSF. For the DA perfusion sessions, after the animal produced the first 20 licks, the aCSF perfusate was switched to aCSF+DA. On these sessions samples were collected every 10 min and analyzed as described before to confirm that the reverse microdialysis was effective.

Electrophysiological recordings and firing rate analysis

Neural electrical activity was recorded from a movable 2 × 8 array of 16 tungsten microwires using a multichannel acquisition processor (Tucker-Davis Technologies). Only single neurons with action potentials of signal-to-noise ratios >3:1 were analyzed. The action potentials were isolated online by means of voltage-time threshold windows and a three-principal components contour templates algorithm. Spikes were resorted using Offline Sorter software (Plexon). Data was then imported into Matlab for analysis using custom-written software. To calculate the firing rate, instantaneous firing rate for was smoothed using Matlab smooth with a 60 s moving average. To test the significance of firing rate changes, we used an individual unit analysis. A one-factor ANOVA was performed on each unit to determine whether the mean firing rate after the I.P. injection (of either Saline or CNO) was significantly different from that before the injection (baseline) and units were classified in three populations: excited, inhibited; and neutral. Finally, an odd-ratio test was performed on those population to determine the change in ratios (CNO:SAL). All recordings were performed in the home cages and the I.P. catheter was used to deliver the I.P. injections. The exterior part of the I.P. catheter was connected to a segment of MicroRenathane tubing secured to the tip of a 1mL standard syringe containing the solutions to be injected and

mounted on the syringe pump. The syringe pump was placed on top of the cage in such a way that mice were able to move freely inside the home cage. The CNO dose was the same used for the behavioural experiments (1mg kg body weight^{-1}). The rate of the injections was calculated in such a way that all injections lasted for 1 min.

Histological Analyses

Mice were sacrificed with a lethal dose of ketamine and xylazine (400 mg ketamine + 20 mg xylazine kg body weight^{-1} I.P.). All animals were transcardially perfused with filtered saline, followed by 4% paraformaldehyde. Following perfusion, brains were left in 4% paraformaldehyde for 24 hours and then moved to a 20% sucrose solution in PBS for 2 days. Brains were then frozen and cut into four series 40 μm sections (either coronal or sagittal) with a sliding microtome equipped with a freezing stage. To identify fibre and electrode locations, relevant sections were identified and mounted on slides. Sections were then photographed under bright field and fluorescence. For c-fos measurements, unilateral stimulation was performed using 1 minute ON/1 minute OFF cycles during 10 minutes. For striatal stimulation 0.5s on/0.5s off cycles were used during the ON cycles, and 10Hz was used for pallidum and *Substantia Nigra* stimulation. 90 minutes after the stimulation protocols mice were sacrificed and perfused as described before.

Fos Expression analyses: To visualize Fos immunoreactivity, we used the ABC/DAB procedure. Briefly, brain sections were first rinsed with 0.02 M potassium phosphate buffer (KPBS, pH 7.4), then immersed into a incubating solution [2% normal goat serum (NGS) and 0.3% Triton X-100 in KPBS] containing a rabbit polyclonal antiserum directed against the N-terminal region of the Fos gene (Ab-5, Calbiochem; dilution 1:10000) and incubated at 4 °C for 36 h. After primary antibody incubation, tissues were washed in 0.02 M KPBS and incubated at room temperature for 2h with goat anti-rabbit, biotinylated secondary IgG (anti-rabbit IgG, Vector Laboratories, 1:200), washed again in 0.02 M KPBS and subsequently reacted for 1 h with avidin-biotin-peroxidase complex (“ABC” method, Vectastain Elite ABC kit, Vector Co) at room temperature. A nickel diaminobenzidine (Nickel-DAB) glucose oxidase reaction was used to visualize Fos-like immunoreactive cells. Finally, sections were washed in KPBS and mounted, air-dried, dehydrated in alcohol, cleared in xylene, and coverslipped.

Fos expression was analysed and quantified as follows: Coronal sections at ~160μm intervals throughout the rostral-caudal extent of the ventral pallidum and the *Substantia Nigra reticulata* were photographed at 10× magnification and montaged with Adobe Photoshop to preserve anatomical landmarks. Fos+ neurons were counted manually on each slice (5 slices per animal for ventral pallidum and 7 slices per animal for substantia nigra reticulata) and expressed as the cumulative sum of Fos+ neurons within the relevant regions for each animal.

Overall Experimental Design and Analysis

Overall design: Data collection and analysis were not performed blind to the conditions of the experiments, due to the nature of most experiments (stereotaxic position of microdialysis probe, laser state ON *vs.* OFF). Data were collected and processed as blocks according to

the experimental conditions. Animals were randomly assigned to the different experimental groups.

Exclusion criteria: No animals that completed the appropriate experimental condition, or any associated data points, were removed from the final analyses. A priori criteria determined that animals showing post-surgical signs of distress or excess weight loss were removed before the completion of the studies. For optogenetic experiments, a priori exclusion criteria related to lack of expression of *Cre*-dependent ChR2 in striatal neurons. One entire group of animals (N=6) was replaced due to lack of ChR2+ expression in any striatal neuron.

Sample sizes: Samples sizes were determined based on our own previous studies employing similar neurochemical, optogenetic and behavioral approaches. Samples sizes adopted in our current study were sufficient for detecting robust effect sizes while complying with guidelines enforcing minimal animal usage and distress.

Statistical Analyses: Data analyses were performed using SPSS (PASW Statistics Release 18.0.0) and Matlab (v.14a, MathWorks). Data distribution was assumed to be normal but this was not formally tested due to normality tests being inconclusive when small sample sizes are employed (normal probability plots instead). Consistently with the overall experimental design and group assignments, statistical analyses only made use of standard linear model (Pearson correlation) analyses as standard well as one- or two-way (repeated measures) ANOVAs and post-hoc t-tests tests whenever relevant. All p-values associated with the t-tests performed correspond to two-tailed tests, and all post-hoc tests were corrected for multiple comparisons by employing Bonferroni correction. All data are reported as mean ±s.e.m. Every experimental group entered in statistical analyses was associated with the corresponding computation of its mean±s.e.m.

Code availability

MED-PC® IV (Med Associates Inc., St. Albans, VT, USA) was used as the platform for programming all experimental schedules involving behavioural and optogenetic protocols. All custom codes employed to generate behavioural and optogenetic data are freely available upon request.

A Supplementary Methods Checklist is available.

Supplementary Material

Refer to Web version on PubMed Central for supplementary material.

Acknowledgments

This work was supported by NIH grants R01DC014859 and R01CA180030 (to I.E.A.); R01 DK103176, DK084052, and NS48476 (to A.vdP.); China Scholarship Council 201206260072 (to W.H.); and FAPESP (Sao Paulo) 2013/09405-3 (to T.L.F.).

References

1. Holman GL. Intragastric reinforcement effect. J Comp Physiol Psychol. 1968; 69:432–441. [PubMed: 5349026]
2. Sclafani A. Post-ingestive positive controls of ingestive behavior. Appetite. 2001; 36:79–83. [PubMed: 11161347]
3. de Araujo IE, Oliveira-Maia AJ, Sotnikova TD, Gainetdinov RR, Caron MG, Nicolelis MA, Simon SA. Food reward in the absence of taste receptor signaling. Neuron. 2008; 57:930–941. [PubMed: 18367093]
4. Zuker CS. Food for the brain. Cell. 2015; 161:9–11. [PubMed: 25815979]
5. Stephenson-Jones M, Kardamakis AA, Robertson B, Grillner S. Independent circuits in the basal ganglia for the evaluation and selection of actions. Proc Natl Acad Sci U S A. 2013; 110:E3670–3679. [PubMed: 24003130]
6. Everitt BJ, Robbins TW. Neural systems of reinforcement for drug addiction: from actions to habits to compulsion. Nat Neurosci. 2005; 8:1481–1489. [PubMed: 16251991]
7. Gerfen CR, Surmeier DJ. Modulation of striatal projection systems by dopamine. Annu Rev Neurosci. 2011; 34:441–466. [PubMed: 21469956]
8. Costa RM. Plastic corticostriatal circuits for action learning: what's dopamine got to do with it? Ann N Y Acad Sci. 2007; 1104:172–191. [PubMed: 17435119]
9. Grillner S, Robertson B, Stephenson-Jones M. The evolutionary origin of the vertebrate basal ganglia and its role in action selection. J Physiol. 2013; 591:5425–5431. [PubMed: 23318875]
10. Yin HH, Ostlund SB, Balleine BW. Reward-guided learning beyond dopamine in the nucleus accumbens: the integrative functions of cortico-basal ganglia networks. Eur J Neurosci. 2008; 28:1437–1448. [PubMed: 18793321]
11. Wickens JR, Horvitz JC, Costa RM, Killcross S. Dopaminergic mechanisms in actions and habits. J Neurosci. 2007; 27:8181–8183. [PubMed: 17670964]
12. Palmiter RD. Dopamine signaling in the dorsal striatum is essential for motivated behaviors: lessons from dopamine-deficient mice. Ann N Y Acad Sci. 2008; 1129:35–46. [PubMed: 18591467]
13. Ren X, Ferreira JG, Zhou L, Shammah-Lagnado SJ, Yeckel CW, De Araujo IE. Nutrient Selection in the Absence of Taste Receptor Signaling. J Neurosci. 2010; 30:8012–8023. [PubMed: 20534849]
14. Roitman MF, Wheeler RA, Carelli RM. Nucleus accumbens neurons are innately tuned for rewarding and aversive taste stimuli, encode their predictors, and are linked to motor output. Neuron. 2005; 45:587–597. [PubMed: 15721244]
15. Hajnal A, Norgren R. Taste pathways that mediate accumbens dopamine release by sapid sucrose. Physiol Behav. 2005; 84:363–369. [PubMed: 15763573]
16. Ericsson J, Stephenson-Jones M, Perez-Fernandez J, Robertson B, Silberberg G, Grillner S. Dopamine differentially modulates the excitability of striatal neurons of the direct and indirect pathways in lamprey. J Neurosci. 2013; 33:8045–8054. [PubMed: 23637194]
17. Planert H, Berger TK, Silberberg G. Membrane properties of striatal direct and indirect pathway neurons in mouse and rat slices and their modulation by dopamine. PLoS One. 2013; 8:e57054. [PubMed: 23469183]
18. Yang CF, Chiang MC, Gray DC, Prabhakaran M, Alvarado M, Juntti SA, Unger EK, Wells JA, Shah NM. Sexually dimorphic neurons in the ventromedial hypothalamus govern mating in both sexes and aggression in males. Cell. 2013; 153:896–909. [PubMed: 23663785]
19. Glendinning JI, Gresack J, Spector AC. A high-throughput screening procedure for identifying mice with aberrant taste and oromotor function. Chem Senses. 2002; 27:461–474. [PubMed: 12052783]
20. Kravitz AV, Tye LD, Kreitzer AC. Distinct roles for direct and indirect pathway striatal neurons in reinforcement. Nat Neurosci. 2012; 15:816–818. [PubMed: 22544310]
21. Lobo MK, Covington HE 3rd, Chaudhury D, Friedman AK, Sun H, Damez-Werno D, Dietz DM, Zaman S, Koo JW, Kennedy PJ, Mouzon E, Mogri M, Neve RL, Deisseroth K, Han MH, Nestler

EJ. Cell type-specific loss of BDNF signaling mimics optogenetic control of cocaine reward. Science. 2010; 330:385–390. [PubMed: 20947769]

22. Cui G, Jun SB, Jin X, Pham MD, Vogel SS, Lovinger DM, Costa RM. Concurrent activation of striatal direct and indirect pathways during action initiation. Nature. 2013; 494:238–242. [PubMed: 23354054]
23. Johnson PM, Kenny PJ. Dopamine D2 receptors in addiction-like reward dysfunction and compulsive eating in obese rats. Nat Neurosci. 2010; 13:635–641. [PubMed: 20348917]
24. DeLong MR, Crutcher MD, Georgopoulos AP. Relations between movement and single cell discharge in the substantia nigra of the behaving monkey. J Neurosci. 1983; 3:1599–1606. [PubMed: 6875659]
25. Wurtz RH, Hikosaka O. Role of the basal ganglia in the initiation of saccadic eye movements. Prog Brain Res. 1986; 64:175–190. [PubMed: 3523602]
26. Sternson SM, Roth BL. Chemogenetic tools to interrogate brain functions. Annu Rev Neurosci. 2014; 37:387–407. [PubMed: 25002280]
27. Dus M, Min S, Keene AC, Lee GY, Suh GS. Taste-independent detection of the caloric content of sugar in Drosophila. Proc Natl Acad Sci U S A. 2011; 108:11644–11649. [PubMed: 21709242]
28. Burke CJ, Huetteroth W, Owald D, Perisse E, Krashes MJ, Das G, Gohl D, Silies M, Certel S, Waddell S. Layered reward signalling through octopamine and dopamine in Drosophila. Nature. 2012
29. Yamagata N, Ichinose T, Aso Y, Placais PY, Friedrich AB, Sima RJ, Preat T, Rubin GM, Tanimoto H. Distinct dopamine neurons mediate reward signals for short- and long-term memories. Proc Natl Acad Sci U S A. 2015; 112:578–583. [PubMed: 25548178]
30. O'Doherty JP. The problem with value. Neurosci Biobehav Rev. 2014; 43:259–268. [PubMed: 24726573]
31. Shammah-Lagnado SJ, Costa MS, Ricardo JA. Afferent connections of the parvocellular reticular formation: a horseradish peroxidase study in the rat. Neuroscience. 1992; 50:403–425. [PubMed: 1279462]

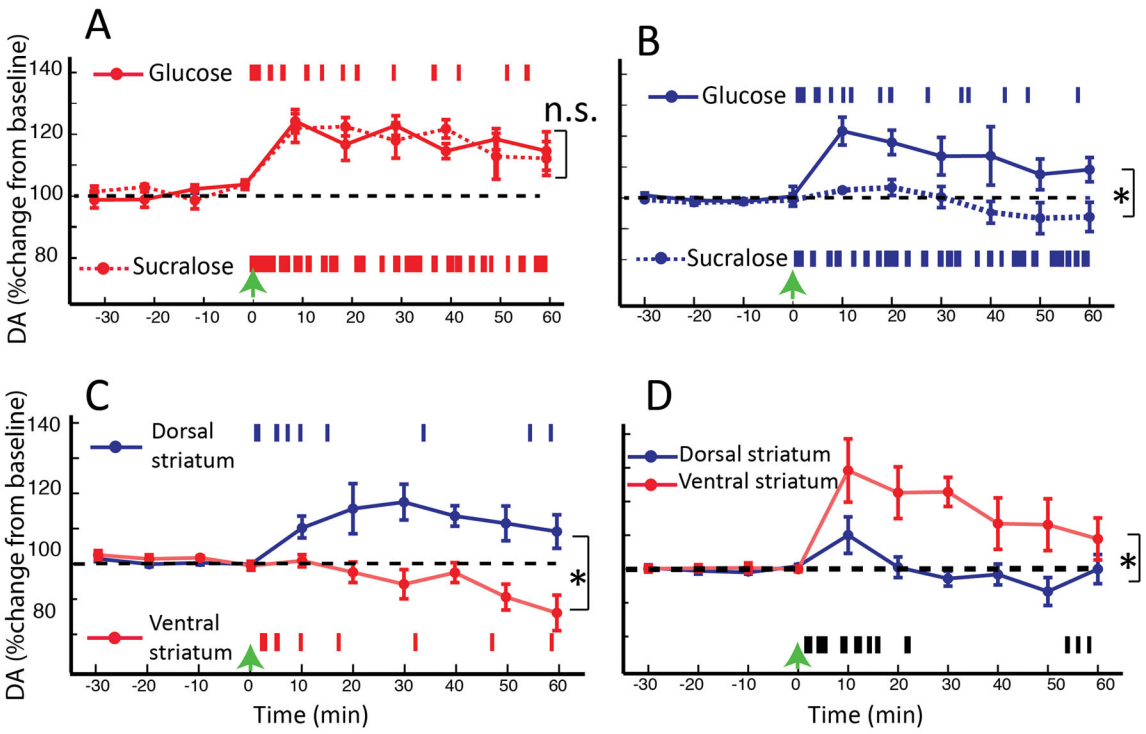

Figure 1. Gustatory and nutritional signals separately control dopamine levels in ventral *versus* dorsal striatum

A. Higher ventral striatal DA levels were observed during sucralose licking upon intra-gastric infusions of both glucose (N=6) and sucralose (N=6, two-way mixed model ANOVA, Sucralose *vs.* glucose effect F[1,4]=0.006, p=0.94). Graph displays changes in DA during the 1h intake session after 30min baseline sampling. Raster plot shows across-animals average lick rates for each (sucralose *vs.* glucose) session type, with total lick counts shown in 10 minutes bins. Onset of licking is shown by green arrow. Sessions involving sucralose infusions are shown as dotted lines, and sessions involving glucose infusions as solid lines. For comparisons against baseline see Supplementary Fig. 1. **B.** Higher dorsal striatal DA levels were observed upon intra-gastric infusions of glucose (N=6) compared to sucralose (N=6, F[1,10]=8.2, *****p=0.017). Note DA levels upon sucralose infusions remained at baseline levels (represented by horizontal dotted line). **C.** Adulteration of the sucralose solution with bitter compound inhibited DA release in VS (n=7) but not DS (n=8, Two-way mixed effects ANOVA, DS *vs.* VS effect F[1,13]=15.7, *****p=0.002). All animals received D-glucose intra-gastric infusions upon licking. **D.** Intra-gastric infusions of non-metabolizable L-glucose inhibited sugar-induced dopamine release in DS but not VS (n=6, Two-way within-subjects ANOVA, DS *vs.* VS effect F[1,5]=13.9, *****p=0.013). VS and DS were sampled simultaneously (licks shown in one raster, dark). DA=dopamine. DS=Dorsal striatum. n.s.=Statistically-non-significant. VS=Ventral striatum.

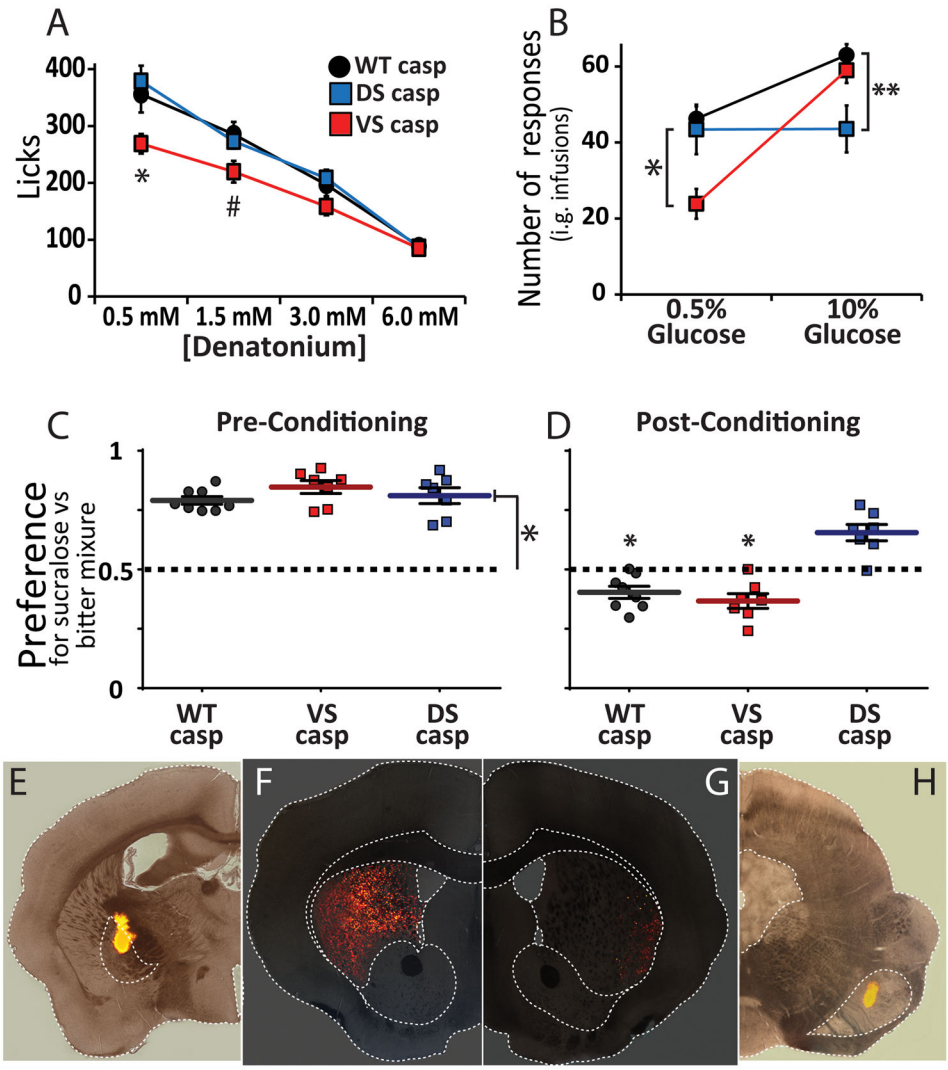

Figure 2. Cell-specific ablation of D1r-neurones in dorsal, but not in ventral, striatum is necessary for sugar-driven consumption of unpalatable solutions

A. Cell-specific ablation of D1r-neurones in VS, but not in DS, increased the sensitivity to unpalatable solutions (Two-way RM-ANOVA, bitterness × lesion site F[6,57]=3.38, p=0.006; group effect F[2,16]=3.59, p=0.048). VS-casp mice were particularly sensitive to the lower concentrations of bitter (One-way ANOVA main effect of lesion F[2,21]=6.19, p=0.008; VS-casp *versus* DS-casp [Bonferroni-corrected *****p=0.013,] or WT-casp control [Bonferroni-corrected *****p=0.029 and #p=0.036] groups. **B.** Cell-specific ablation of D1r-neurones in DS, but not VS, abolished sugar-induced consumption of unpalatable solutions (Two-way RM-ANOVA, glucose concentration × lesion site effect F[2,19]=11.2, p=0.001; lesion site effect F[2,19]=4.4, p=0.027; glucose concentration effect F[1,19]=32.12, p=0.000018). Note that in the non-nutritive (0.5% glucose) condition ventrally-lesioned VS-casp mice are more sensitive to bitterness than both control WT-casp and dorsally-lesioned DS-casp mice (One-way ANOVA group effect F[2,21]=7.07, p=0.005; VS-casp *versus* DS-casp [Bonferroni-corrected *****p=0.023] and WT-casp [Bonferroni-corrected *****p=0.007]. This effect was completely reversed by increasing the glucose concentration to nutritive levels,

such that DS-casp mice failed to display the similar increases in responding (One-way ANOVA group effect F[2,21]=7.09, p=0.005; DS-casp *versus* VS-casp [Bonferroni-corrected **p=0.024] and WT-casp [Bonferroni-corrected **p=0.007]. **C.** Taste-nutrient learning. Three groups of sugar/sweet naïve, food-restricted mice (WT-casp, N=8; DS-casp, N=7; and VS-casp, N=7) were exposed to short-access 5-min two-bottle test between sucralose and an adulterated bitter/sucralose mix. As expected, all groups strongly preferred sucralose to the bitter mix (one-sample t tests against indifference ratio of 0.5, marked as red horizontal dotted line: WT-casp, *p=0.0000012; DS-casp, *p=0.00026; VS-casp, *p=0.000042]. **D.** Next, the animals were exposed to 1h conditioning one-bottle sessions where intake of the bitter mixture was paired to intra-gastric infusions of D-glucose, and intake of sucralose was paired to intra-gastric infusions of sucralose. Following the conditioning sessions, while WT-casp [Bonferroni-corrected *p=0.036] and VS-casp [Bonferroni-corrected *p=0.045] mice shifted preferences away from sweetness towards the nutritive bitter taste, DS-casp mice failed to shift preferences in response to gut glucose sensing [preference for sucralose > bitter mix, p=0.074]. **EH.** When Retrobeads were injected into *globus pallidus* (GP, dotted line in **G**, targeted by D2r-expressing neurons of DS) of DS-casp mice, strong labeling was observed throughout DS (**F**). In contrast, weak labelling was observed in DS (**G**) when Retrobeads were injected into SNr, on the opposite hemisphere to the one receiving a Retrobeads deposit in GP (dotted line in **H**). SNr is exclusively targeted by D1r-expressing neurons of DS. The same fluorescence (or lack thereof) pattern was observed in all animals sustaining the same injections. *Abbreviations*: DS-casp: Caspase-driven D1r-dependent lesions in DS of D1r-*Cre* mice (N=7); VS-casp: Caspase-driven D1r-depedent lesions in VS of D1r-*Cre* mice (N=7); WT-casp: Viral delivery of *Cre*-dependent caspase in DS/VS of non-*Cre* mice (N=8). n.s. = non-statistically significant.

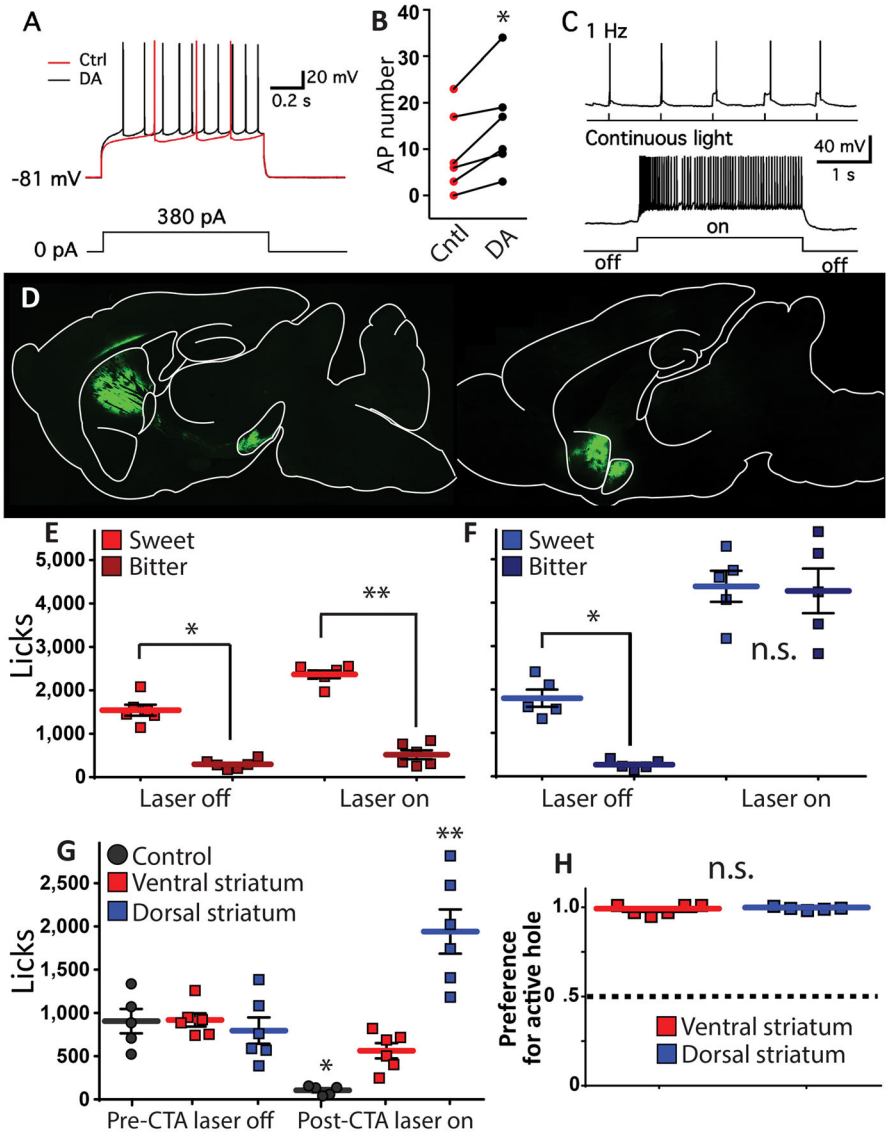

Figure 3. Optogenetic stimulation of D1r-neurones in dorsal, but not in ventral, striatum substitutes for sugar in driving consumption of unpalatable solutions

A. Representative traces showing DS D1r-neurone firing as evoked by a depolarizing current injection (380 pA, 1s) in the presence of dopamine (30μM, black) and control (shown in red) solutions. **B.** Mean action potential (AP) counts during 1s depolarization in the presence of dopamine and control solutions (N=6, paired t-test, *****p=0.013). **C.** Optogenetic activation of a ChR2+ D1r-neurone by 1Hz blue light pulses (10ms) and by a continuous light train (see additional analyses in Supplementary Fig. 4). This experiment was successfully replicated in 10 cells sampled from two mice. **D.** EYFP visualization confirms that ChR2 transfection was contained to VS and DS. Note the dense bundle of axon terminals in VP and SNr, respectively. Panels are composites of sequential 10× images of one entire sagital section. The same fluorescence pattern is observed in all six animals sustaining the same injections. **E.** In animals transfected with ChR2 in VS, adulteration of the sucralose solution by the bitter toxin produced a drastic decrease in intake (Laser OFF, N=6, paired T-test sweet *vs.*

bitter t[5]=10.03, *****p=0.0002) that was not reversed by D1r-neurone optogenetic stimulation (Laser ON: t[5]=10.5, *****p=0.0001). **F.** In animals transfected with ChR2 in DS, adulteration of the sucralose solution produced a drastic decrease in intake (Laser OFF, N=5, t[4]=7.24, *p=0.002) that was nevertheless totally reversed by D1r-neurone optogenetic stimulation (Laser ON: t[4]=0.28, p=0.79). **G.** Conditioned sweet taste aversion (CTA) induced by visceral malaise decreased intake in control (ChR2-negative) mice (sweetener intake pre- *vs.* post-malaise N=5, paired t-test t[4]=5.76, Bonferroni *****p=0.01). Mice transfected with ChR2 in VS failed to increase intake despite laser stimulation (N=6, t[5]=2.7, Bonferroni p=0.1). However, laser stimulation of DS markedly increased intake despite conditioned aversion (N=6, t[5]=4.5, Bonferroni ******p=0.01). Overall group effect F[2,14]=13.1, p=0.001. **H.** Optogenetic self-stimulation of VS and DS as triggered by nose pokes (in the absence of food cues) produced equal numbers of pokes in the active *vs.* inactive holes (ratio between pokes in active *vs.* inactive holes is shown, DS (N=5) *vs.* VS (N=6) effect t[9]=0.76, p=0.47).

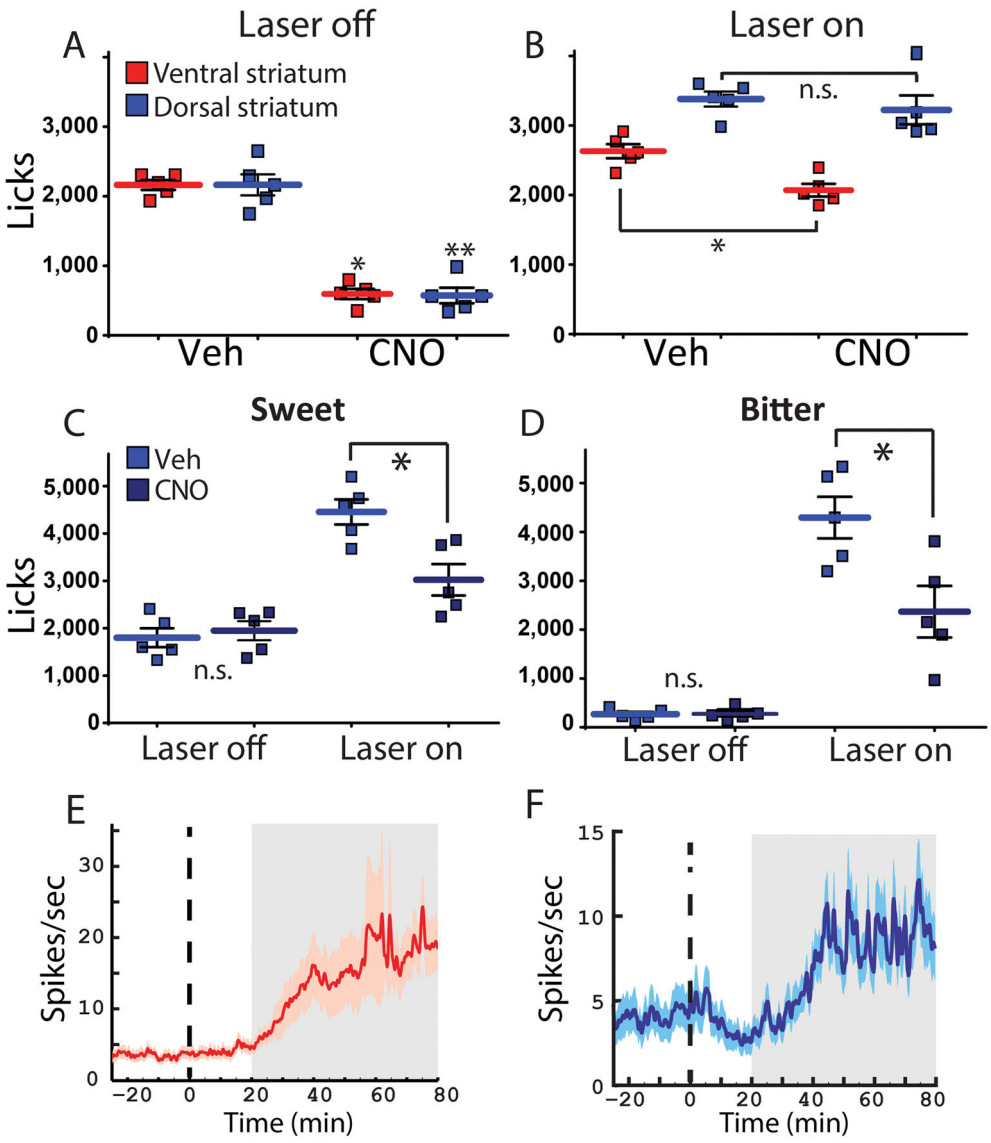

Figure 4. The dorsal striato-nigral pathway overrides inhibitory signals released by ventral output regions

We employed a combination of optogenetics and DREADDS. Animals expressed the designer receptor hM3D(Gq) in either VP or SNr (DREADD denoted by syringes in relevant locations, see scheme in Supplementary Fig. 8). One group of animals ("VS=>VP pathway") was ChR2-tranfected in VS, and optical fibres placed immediately above the D1r-neurone terminals in VP (N=5). A second group of animals ("DS=>SNr pathway") was ChR2-tranfected in DS, and optical fibres placed immediately above the D1r-neurone terminals in SNr (N=5). **A.** In the absence of light pulses, CNO administration robustly suppressed sweetener intake in both groups (VS=>VP group, CNO *vs.* saline effect paired t-test t[4]=14.54, Bonferroni ***p=0.00052; DS=>SNr group, t[4]=8.45, ****p=0.004). **B.** Optogenetic activation of VS=>VP terminals produced an increase in sweetener intake that was annulled by activating VP with CNO (t[4]=5.37, Bonferroni ***p=0.024). However, activating VP with CNO produced no effects on the robust increases in sweetener intake

associated with optogenetically activating DS=>SNr terminals (t[4]=0.98, p=0.38). **C.** To assess pathway-specificity, one additional group of animals expressed hM3D(Gq) in SNr instead of VP. ChR2 was tranfected in DS, and optical fibres were placed immediately above the D1r-neurone terminals in SNr. Optogenetic activation of DS=>SNr terminals produced an increase in sweetener intake that was weakened by activating SNr with CNO (t[4]=4.8, *****p=0.0083). CNO alone had no effect (p=0.60). **D.** Optogenetic activation of DS=>SNr terminals produced a robust increase in bitter intake that was weakened by activating SNr with CNO. Paired sample t-test 2-tailed t[4]=6.6, *p=0.0027. CNO alone had no effect, t[4]=0.3, p=0.79. Reliable activation of hM3D(Gq)-transfected neurones in VP (**E)** and SNr (**F)** by administration of the designer drug clozapine-N-oxide (CNO) was confirmed *in vivo* using multi-channel electrophysiological recordings. Dotted line represents onset of CNO injections. Graph shows average firing rate activity over sessions. Shadowed area around trace represents s.e.m. n.s.= Statistically non-significant.